This is an *Accepted Manuscript*, which has been through the Royal Society of Chemistry peer review process and has been accepted for publication.

Accepted Manuscripts are published online shortly after acceptance, before technical editing, formatting and proof reading. Using this free service, authors can make their results available to the community, in citable form, before we publish the edited article. We will replace this *Accepted Manuscript* with the edited and formatted *Advance Article* as soon as it is available.

You can find more information about *Accepted Manuscripts* in the **Information for Authors**.

Please note that technical editing may introduce minor changes to the text and/or graphics, which may alter content. The journal's standard **Terms & Conditions** and the **Ethical guidelines** still apply. In no event shall the Royal Society of Chemistry be held responsible for any errors or omissions in this *Accepted Manuscript* or any consequences arising from the use of any information it contains.

All-metal electride molecules CuAg@Ca₇M (M = Be, Mg, and Ca) with multi-excess electrons and all-metal polyanions: molecular structures and bonding modes as well as large infrared nonlinear optical responses

Hui-Min He[a], Ying Li[a], Wei-Ming Sun[a, c], Jia-Jun Wang[a, b], Di Wu[a*], Rong-Lin Zhong[a], Zhong-Jun Zhou[a], Zhi-Ru Li[a*]

[a] *Institute of Theoretical Chemistry, Jilin University, Changchun 130023, P. R. China*

[b] *Key Laboratory of Preparation and Application of Environmental Friendly Materials, Ministry of Education, College of Chemistry, Jilin Normal University, Haifeng Road No.1301, Siping City,Jilin Provience. 136000, P. R. China*

[c] *Department of Basic Chemistry, Faculty of Pharmacy, Fujian Medical University, Fuzhou, Fujian 350108, P R China*

Abstract

All-metal electride molecules CuAg@Ca₇M (M = Be, Mg and Ca) are designed and researched in theory for the first time. In these molecules, a pull-push electron relay occurs. Unusual all-metal polyanions of fourfold negatively charged $[Cu-Ag-Be/Mg]^{4-}$ and $[Cu-Ag]^{4-}$ with 4 extra electrons gained from Ca atoms, push the remaining valence electrons of the Ca atoms forming the multi-excess electrons (Ne=10/12). Therefore, these molecules can be described as salt-like $[(Ca^{2+})_7(CuAgM)^{4-}]+10e^-$ (M = Be and Mg) and $[(Ca^{2+})_8(CuAg)^{4-}]+12e^-$. In these salt-like molecules, there are extraordinary covalent bonding modes including 2c-2e/3c-2e σ-bonding in the polyanions and the Ca^{2+} cations sharing the diffuse multi-excess electrons.

For intriguing nonlinear optical (NLO) response, these all-metal electride molecules display large electronic first hyperpolarizabilities (β_0), thus a new class of NLO molecules – all-metal electride NLO molecules emerge. Meanwhile, it is also found that manipulating atomic number and position of M is a new strategy to enhance β_0. As a result, the CuAg@Ca₇Mg(1) exhibits considerable β_0 (1.43×10^4 au) being 16 times the β_0 sum of two isolated CuAg and Ca₇Mg(1) subunits, which deeply reveals the fundamental origin of considerable β_0, namely the multi-excess electrons generated by subunit interaction. These all-metal electride molecules have the infrared (IR) transparent region of 1.3-6 μm, and hence are new IR NLO molecules. Besides electronic contribution β_0, the large effects of vibrations

*Corresponding author.
Email address: lzr@jlu.edu.cn
*Corresponding author.
Email address: wud@mail.jlu.edu.cn

on static first hyperpolarizabilities of these all-metal electride molecules are also estimated. Thus, this work opens a new research field of all-metal electride IR NLO molecule.

1. Introduction

In recent years, a new research field of NLO molecules has been established since it is discovered that introducing the excess electron into a molecule is an effective approach to remarkably enhance the static first hyperpolarizability (β_0).[1-2] Especially, the electride molecule[3-10] including the excess electron anion has attracted great attention. In previous works, it has been found that the alkali-metal-atom-doped molecules with cup-like,[11] cage-like,[12-13] and chain-like[14] complexants exhibited large first hyperpolarizabilities due to the excess electron generated by the push/pull electron effect of the complexants in these systems.[15] More recently, a series of new strategies for enhancing the NLO response and electronic stability have been proposed for electride molecules. These strategies include regulating the behaviors of pushed and pulled electron, size, shape, and the number of coordination site of complexants,[15] as well as the number and spin state of excess electrons to manipulate excess electron binding state[16] in the electride molecules. It is noteworthy that although the electride molecules usually possess satisfactory β_0, they have not a transparent infrared (IR) region of electronic spectra. Thus, they are not the expected IR NLO electride molecules yet.

IR NLO materials are widely used in modern laser frequency conversion technology and optical parameter oscillator processes.[17-20] High performance IR NLO crystals are rare, and each of the commercial crystals unfortunately suffers its own drawbacks (low laser damage threshold and so on), which hinders their application. Therefore, the exploration and development of new IR NLO compounds[21-23] is of broad scientific and technological importance.[24]

Fortunately, although constructing new electride molecules with large IR NLO response is a great challenge for NLO molecule design, unusual all-metal polyanions can be used here as novel structural units with interesting bonding features in the chemistry of the polar intermetallic compound.[25-29] Specially, all-metal extended Zintl polyanions[30-34] have the capacity to push the electrons of the electron donor to form excess electrons, which leads to the formation of a new class of compounds. For transition-metal anions among the late 3d or 4d elements, thier $d^{10}s^2p^1$ case is found for reported compounds containing $[Pt-Pt]^{6-}$, $[Au-Au]^{4-}$, $[Ag-Ag]^{4-}$, and $[Cu-Cu]^{4-}$ dimer anions[35-37]. Synthetised Ca_5Ag_3 and Ca_5Au_3 containing $(Ag-Ag)^{4-}(Ag^{2-})$ and $(Au-Au)^{4-}(Au^{2-})$[38-39], their electronic structure[30] can be described as $[(Ca^{2+})_5(Ag-Ag)^{4-}(Ag^{2-})]+4e^-$ and $[(Ca^{2+})_5(Au-Au)^{4-}(Au^{2-})]+4e^-$. This new class of compounds not only has electride feature due to containing excess electron anions but also has an all-metal composition characteristic. Thus, we propose a new concept "all-metal electride" to describe the novel intermetallic compounds containing excess electron anions.

In order to construct new IR NLO molecules of all-metal electride, alkaline earth metal calcium atom is selected to serve as the electron source. In other words, all-metal extended Zintl polyanions are

formed by gaining some valence electrons from Ca atoms and in turn push the remaining valence electrons of Ca atoms to form the excess electrons. Different from the previously reported NLO materials (containing non-metal elements) being insulators or semiconductors, all-metal electride molecules have electrical conductivity due to the existence of multi-excess electrons. Consequently, a potential phenomenon – electric current effect on NLO responses may be predicted.

In this paper, we further consider substituting Be and Mg for one Ca atom to construct novel all-metal electride molecules CuAg@Ca$_7$M (M = Be, Mg, and Ca). The evolutions of structure and properties as well as stability of the CuAg@Ca$_7$M molecules are shown. In addition, extraordinary polar metal-metal bonds in the all-metal electride molecules are also discussed. Especially, the large NLO responses and IR transparent optical spectrum region of these novel electride molecules are revealed. This work will open new perspective for the development of novel all-metal electride NLO molecules.

2. Computational details

For computational methods, density functional theory (DFT) has now become the preferred method for complex chemical systems including transition metals.[40] For the applications of density functionals to molecular structures containing transition metals (groups 3 to 12 on the periodic table)[41-42], the exact-exchange-incorporated PBE0 is the most satisfactory functional.[43-47]

The choice of suitable basis sets for molecular structure and property calculations is another major issue in modern computational quantum chemistry. For predicting geometric structures and physicochemical properties of transition metal systems, the Los Alamos set of the double-zeta type LANL2DZ[48-50] for transition metals and Pople-type basis sets for the others have been proved to be competent.[51] As for accurately calculating the electronic first hyperpolarizabilities, the studies of the basis set effect[52-57] show the importance of embedding diffuse basis functions. And basis set choices have been discussed in detail for electride[58], open-shell π-conjugated systems[59-61], and singlet diradical systems.[62]

As our systems contain the transition elements, the PBE0 functional is selected here. Hence, the optimum geometric structure and vibrational frequency calculations were performed for all-metal electride molecules CuAg@Ca$_7$M (M = Be, Mg and Ca) at the PBE0 level. The natural bond orbital (NBO)[63] analyses, vertical ionization potential (VIP) and binding energy (E_b) calculations were also performed at the PBE0 level. Meanwhile, the LANL2DZ for Cu and Ag and the 6-31G(3df) basis set for Be, Mg and Ca were employed. The binding energy of the M atom is calculated by counterpoise procedure[64-65] and defined as:

$$E_b = E_A + E_B - E_{AB} \qquad (1)$$

where the same basis set, X$_{AB}$, was used for the subunit energy (E_A and E_B) calculation as for the compound energy (E_{AB}) calculation.

The first electronic hyperpolarizabilities (β_0) of five electride molecules were calculated by the high level MP2 method[66-67] in conjunction with the LANL2DZ for Cu and Ag and the 6-311+G(3df) basis set for Be, Mg and Ca (The studies of the basis set effect are shown in Table S1 and Table S2). The static first hyperpolarizability (β_0) and dipole moment (μ_0) are noted as follows:

$$\beta_0 = (\beta_x^2 + \beta_y^2 + \beta_z^2)^{1/2}$$

(2)

where

$$\beta_i = \frac{3}{5}(\beta_{iii} + \beta_{ijj} + \beta_{ikk}), \text{ i, j, k = x, y, z}$$

$$\mu_0 = (\mu_x^2 + \mu_y^2 + \mu_z^2)^{1/2}$$

(3)

All of the calculations were carried out using the GAUSSIAN09 program package.[68] Molecular orbitals were visualized with the GaussView program.[69]

3. Results and discussion

3.1 Equilibrium geometries

The five optimized structures of CuAg@Ca$_7$M (M = Be, Mg and Ca) with all real frequencies are exhibited in Figure 1. In the optimized structure of CuAg@Ca$_8$, two square four-membered rings (Ca(1)Ca(2)Ca(7)Ca(8) and Ca(3)Ca(4)Ca(5)Ca(6)) form a quasi-cube with the C4 axis passing through a Cu-Ag bond. In the Cu-Ag bond, the Ag atom is sandwiched between the two staggered four-membered rings but Cu atom locates slightly under the quasi-cube (the Cu atom caps on the bottom face of the quasi-cube, see Figure 1).

When a Ca atom is substituted by one Be or Mg atom, the C$_{4v}$ geometry of quondam CuAg@Ca$_8$ is distorted. Obviously, the Be-substitution leads to greater geometric distortions than Mg-substitution does due to the atomic radius order[70] of 1.05 for Be < 1.50 for Mg < 1.80 Å for Ca. Considering M(1)-substitution in the upper four-membered ring, as the M(1)-Ag distance increases in the order 2.540 (Be-Ag) < 2.932 (Mg-Ag) < 3.231 Å (Ca-Ag) (see Table 1), the vertex atom M(1) is gradually pulled toward the Ag atom with decreasing atomic radius of M(1). The order of M(1)-Ca(3 or 6) distances is 2.912/3.089 (Be-Ca) < 3.372 (Mg-Ca) < 3.874 Å (Ca-Ca), the vertex atom M(1) is also gradually pulled down toward the Ca(3)Ca(6) of the bottom ring with decreasing atomic radius of M(1). Thus, the vertex atom M(1) is contracted inward and collapsed down gradually along with its decreasing atomic radius. Considering M(3)-substitution in the lower four-membered ring, as the order of M(3)-Cu distance is 2.130 (Be-Cu) < 2.706 (Mg-Cu) < 2.989 Å (Ca-Cu) (see Table 1), the vertex atom M(3) is gradually pulled toward the Cu atom with decreasing atomic radius of M(3). As the order of M(3)-Ca(1 or 8) distances is 2.983/2.862 (Be-Ca) < 3.479 (Mg-Ca) < 3.874 Å (Ca-Ca), the vertex atom M(3) is gradually pulled up toward the Ca(1)Ca(8) of the upper ring with decreasing atomic radius

of M(3). Then, the vertex atom M(3) is contracted inward and uplifted gradually along with its decreasing atomic radius.

As stated above, M-substitution effects (M = Mg, Be) generate some obvious shorter bond lengths including the Be(1)-Ag (2.540 Å), Be(3)-Cu (2.130 Å) and Be/Mg-Ca bonds (2.862-3.372 Å), compared with corresponding Ca-Ag, Ca-Cu and Ca-Ca bonds in the structure of $CuAg@Ca_8$, respectively. These shorter bonds lead to not only great geometric distortion but also the changes of electronic structure and interatomic bonding.

3.2 Electride characteristic of the intermetallic compounds

Using alkaline earth Ca atoms as the electron sources, and the resulting polyanions $[Cu-Ag]^{4-}$ and $[Cu-Ag-M]^{4-}$ (M = Be and Mg) as electron-pushing subunits, we design the new all-metal electride molecules. The NBO charges (q), valences (V) of anions and polyanions as well as molecular excess electron number (Ne) are shown in Table 2. For the $CuAg@Ca_8$, we can see that the [Cu-Ag] subunit is negatively charged with -3.557|e| charge, indicating that the valence of the [Cu-Ag] subunit is -4. Considering counting the number of electrons, the 8 calcium atoms provide 16 valence electrons. Thereinto, 4 electrons are taken away by [Cu-Ag] forming polyanion $[Cu-Ag]^{4-}$, and the remaining 12 valence electrons are pushed by $[Cu-Ag]^{4-}$ forming the excess electrons of Ne = 12. Figure 2 illustrates the 6 frontier orbitals occupied by the 12 excess electrons (HOMO, HOMO-1, HOMO-2, HOMO-3, HOMO-6, and HOMO-7), showing pushed orbital lobes.

When a calcium atom is substituted with one Be or Mg atom with larger electronegativity, the remaining 7 Ca atoms act as electron source and provide 14 valence electrons. From Table 2, the NBO charges of Mg atoms are close to 0, that is, Mg atoms neither accept nor donate electron. In the Be-substituted molecules, due to the larger electronegativity of Be atom, all of the Be atoms have the charges of ca. -1|e|, suggesting that each Be atom in the molecules accepts one valence electron from Ca atoms.

In the $CuAg@Ca_7M$ (M = Be and Mg), all of the [Cu-Ag-Be/Mg] subunits are negatively charged with -4.112~-3.440|e| (far above -3) charges, which indicates that the valences of [Cu-Ag-Be/Mg] subunits are -4. It is well known that the charge calculated is very closer to valence number of ion, which is not often. Fortunately, in this work, charge calculated is closer to valence number of ion. Two nearest charges, -3.557 and -3.440 are far above -3. They corresponding to -4 valence may be reasonable. For -3 valence, good charge should be -2 – -3. Therefore, for the 14 valence electrons of Ca atoms, the formed polyanion $[Cu-Ag-Be/Mg]^{4-}$ occupied 4 of them. Owing to the repulsion from polyanion $[Cu-Ag-Be/Mg]^{4-}$, the remaining 10 valence electrons of Ca atoms convert into 10 excess electrons occupying excess electron orbitals of 5/6 (see Figure 2, the H-1 and H-5 orbitals have a half of the character of excess electron orbital for M = Mg(1)).

It is noteworthy that owing to including multi-excess electrons (10/12) and unusual metal

polyanions $[Cu-Ag]^{4-}$ and $[Cu-Ag-Be/Mg]^{4-}$, the electronic structures of $CuAg@Ca_8$ and $CuAg@Ca_7M$ (M = Be, Mg) intermetallic compounds can be interestingly described as $[(Ca^{2+})_8(CuAg)^{4-}]+12e^-$ and $[(Ca^{2+})_7(CuAgM)^{4-}]+10e-$ (M = Be and Mg), respectively. Naturally, these intermetallic compounds can be considered as electride molecules with excess electron anions. Actually, some synthesized intermetallic compounds[22,39,71] belong to this case due to containing all-metal zintl anion and alkali or alkali earth metal cations as well as excess electron anions. Then, a new concept of "all-metal electride" is needed and should be presented to describe the unusual intermetallic compound containing excess electron anion. Meanwhile, an interdiscipline of intermetallic compound and electride is beginning.

3.3 Unusual bonding features and molecular stabilities

In these all-metal electride molecules, the resulting all-metal polyanions are also unreported. The covalent bonding in the all-metal polyanions is interesting. Figure 3 illustrates the s-type bonding molecular orbitals in polyanions.

For the bimetallic polyanion $[Cu-Ag]^{4-}$ in $CuAg@Ca_8$, the Cu^{2-} and Ag^{2-} transition metal anions form a two-centre two-electron (2c-2e) σ-bonding. The σ-bond between Cu and Ag anions has the calculated bond length of 2.594 Å and covalent bond order (Wiberg Bond Index ,WBI) value of 0.79 (see Table 1). Of course, owing to surrounding counterions ($8Ca^{2+}$), the possible Coulomb explosion (the charge dissociation of polyion)[72-73] of the polyanion $[Cu-Ag]^{4-}$ is prevented, which is beneficial to forming the σ-bond.

For the trimetallic polyanions $[Cu-Ag-M]^{4-}$ in the M-substituted $CuAg@Ca_7M$ molecules, the covalent bonding modes among Cu, Ag and M elements are 3c-2e σ-bonding. (see Figure 3) As far as the M-substitution effect on 3c-2e σ-bonding is concerned, the M(1) and M(3) positions are considered separately because of their different atomic environments. For M(1)-substitution, in $[Cu-Ag-Be(1)]^{4-}$, the formed 3c-2e σ-bonding of Cu-Ag-Be chain has the Cu-Ag distance of 2.695 Å with the WBI of 0.67 and Ag-Be distance of 2.540 Å with the WBI of 0.65. In $[Cu-Ag-Mg(1)]^{4-}$, the 3c-2e σ-bonding of Cu-Ag-Mg chain has the Cu-Ag distance of 2.594 Å with large WBI of 0.73 and Ag-Mg distance of 2.932 Å with the WBI of 0.44. The difference between the σ-bonding of Cu-Ag-Be(1) and Cu-Ag-Mg(1) chain exhibits an atomic number dependence on M(1).

For M(3)-substitution, in $[Cu-Ag-Be(3)]^{4-}$, the 3c-2e σ-bonding of Cu-Ag-Be triangle has the Cu-Ag distance of 2.763 Å with the WBI of 0.41, Ag-Be distance of 2.636 Å with the WBI of 0.53 and Be-Cu distance of 2.13 Å with large WBI of 0.85. In $[Cu-Ag-Mg(3)]^{4-}$, the 3c-2e σ-bonding of Cu-Ag-Mg triangle exhibits the Cu-Ag distance of 2.621 Å with large WBI of 0.70, Ag-Mg distance of 2.992 Å with the WBI of 0.42 and Mg-Cu distance of 2.706 Å with the WBI of 0.52. The difference between the σ-bonding of Cu-Ag-Be(3) and Cu-Ag-Mg(3) triangle also shows an atomic number dependence on M(3).

In summary, in all-metal polyanions, there are three covalent bonding modes: 2c-2e σ-bonding of

linear Cu-Ag in bimetallic $[Cu-Ag]^{4-}$, 3c-2e σ-bonding of Cu-Ag-M(1) chain in trimetallic $[Cu-Ag-M(1)]^{4-}$ for M(1)-substitution and 3c-2e σ-bonding of Cu-Ag-M(3) triangle in $[Cu-Ag-M(3)]^{4-}$ for M(3)-substitution.

In the all-metal electride molecules, for polar metal-metal bond between oppositely charged atoms, besides Coulombic force of attraction, based on covalent bond order analysis, the extended covalent bonding (sharing electron cloud) feature between individual anions (in $[Cu-Ag-M]^{4-}$ metal polyanions) and the surrounding Ca^{2+} cations have been shown (see WBI values in Table 1). For example, $Ca^{2+}-Ag^{2-}$ having the bond length of 3.111 Å and WBI of 0.61, and $Ca^{2+}-Cu^{2-}$ having the bond length of 2.928 Å and WBI of 0.50 in $CuAg@Ca_7Mg(1)$ are shown. In $CuAg@Ca_7Be(1)$, $Ca^{2+}-Be^{-}$ having the bond length of 2.912 Å and WBI of 0.53 is also exhibited.

Besides, the weakly covalent bonding between Ca^{2+} cations also occurs (see Table 1). The strongest $Ca^{2+}-Ca^{2+}$ bonding in $CuAg@Ca_7Be(3)$ has the WBI of 0.40. In general, for these all-metal electride molecules, the $Ca^{2+}-Ca^{2+}$ bonding has WBIs of 0.18-0.40, which indicates that the novel covalent bonding between Ca^{2+} cations exists. Why? For these unusual molecules with novel endohedral sandwich structure and the Coulomb interaction among layers, the inner all-metal polyanion is surrounded by 7 or 8 Ca^{2+} cations, and the whole framework is surrounded by multi-excess electrons (10 or 12). The diffuse multi-excess electrons surrounding the Ca^{2+} cations as unusual bonding electrons are shared by those Ca^{2+} cations forming extended covalent bonding effect.

As mentioned above, the M-substitution not only generates various 3c-2e σ-bonding modes in the polyanions $[Cu-Ag-Be/Mg]^{4-}$, but also changes the covalent bonding between the anions (in the polyanion) and the surrounding Ca^{2+} cations, as well as novel covalent bonding effect between Ca^{2+} cations.

For molecular stabilities, as is well-known, the gap between the highest occupied molecular orbital (HOMO) and the lowest unoccupied molecular orbital (LUMO) is a useful quantity for examining the chemical stability of molecules. A large gap value reflects a high chemical stability. Table 3 lists the HOMO–LUMO (H-L) gaps of the $CuAg@Ca_7M$ (M = Be, Mg and Ca) all-metal electride molecules. Obviously, the chemical stability order is $CuAg@Ca_7Be(1) < CuAg@Ca_7Be(3) < CuAg@Ca_7Mg(3) < CuAg@Ca_8 < CuAg@Ca_7Mg(1)$. The gaps of the all-metal electride molecules $CuAg@Ca_7M$ (M = Be, Mg and Ca) are in the range of 3.344–3.586 eV, which are larger than those of 1.64 eV for organic electride $Li@3^6Adz$[74], 1.660 eV for $LiCNLi@BNNT$ with excess electron protected inside the nanotube[75], 2.814 eV for $Ca(NH_3)_6Na_2(b'')$[76] and are close to 3.563 eV for $K{\cdots}2C8(O)$[77] with excess electron protected inside the two C8 cage units. Compared to H-L gaps of all-metal clusters, our values are larger than those of 1.03 or 0.99 eV for the clusters with interstitial La ion[78] and 1.80eV for Au_{20} (Td)[79]. Above all, it is shown that these studied all-metal electride molecules have higher chemical stability.

For these electride molecules, the electron stability is important due to the existence of loosely-bound excess electrons. The electron stability of a molecule may be characterized by its VIP value. From Table 2, VIP values of 4.23-4.40 eV for the five all-metal electride molecules are slightly larger than reported values of electride molecules: 3.880 for $Ca@(NH_3)_6Na_2(b'')$,[76] 4.16 for Li@calix[4]pyrrole[10], 4.20 eV for LiCNLi@BNNT[75]. While very large VIP value of 7.78 eV for $Cup\cdots K_3O^+\cdots e@C_{36}F_{36}^-$[80] occurs due to the fact that excess electron is protected inside the $C_{36}F_{36}$ cage with sufficient interior electron attractive potential. It shows that these all-metal electride molecules exhibit moderate electron stability in electride molecules. Considering their stabilizations, anti-oxidation is still needed due to the existence of loosely-bound excess electrons.

To explore the thermostability of the studied molecules, the binding energy (E_b) of an atom (except for Cu and Ag) in the five all-metal electride molecules are obtained at the PBE0 level with counterpoise procedure, as shown in Figure 4 and Table S3. Then, we use the smallest E_b of molecule to represent molecular thermostability. For non-substituted $CuAg@Ca_8$, the smallest E_b is 30 kcal/mol. For the M(1)-substitution cases, Be(1)-substitution generates not only the largest E_b of 52 kcal/mol for Be(1) but also the smallest E_b of 27 kcal/mol for the neighbouring Ca(2), and Mg(1)-substitution generates the smallest E_b of 26 kcal/mol of Mg(1). For the M(3)- substitution cases, Be(3)-substitution generates the smallest E_b of 33 kcal/mol of Ca(7), and then Mg(3)-substitution generates the smallest E_b of 30 kcal/mol of Ca(2) and Ca(7). Obviously, the difference of smallest E_b among these molecules is less than 7 kcal/mol. Consequently, the thermostability order is $CuAg@Ca_7Mg(1) \sim CuAg@Ca_7Be(1) < CuAg@Ca_7Mg(3) = CuAg@Ca_8 \sim CuAg@Ca_7Be(3)$.

3.4 Static first hyperpolarizabilities

Table 3 shows the electric first hyperpolarizabilities (β_0) of the five all-metal electride molecules at the MP2 level. From Table 3, the order of β_0 values is 6500 for non- substituted $CuAg@Ca_8 < 7300$ for $CuAg@Ca_7Mg(3) < 9300$ for $CuAg@Ca_7Be(3) < 12000$ for $CuAg@Ca_7Be(1) < 14300$ au for $CuAg@Ca_7Mg(1)$. Obviously, these novel all-metal electride molecules display large first hyperpolarizabilities (β_0), thus these all-metal electride molecule is a new class of NLO molecules and can be referred to as all-metal electride NLO molecule.

We now discuss the effect of substituting Be or Mg for Ca atom on β_0. It is obviously seen from Figure 5 that Be/Mg-substitution increases β_0 value compared to non-substituted $CuAg@Ca_8$ with the smallest β_0 value. As to substitution position effect on β_0, it is found that the β_0 values of M(3)-substituted molecules (M(3) near Cu) are smaller than those of M(1)-substituted molecules (M(1) near Ag). Considering atomic number effect on β_0, the order of β_0 is Be(1)-substituted molecule < Mg(1)-substituted molecule, but the order of β_0 is inverse for M(3)-substitution. Based on above discussions, a strategy to enhance β_0 is obtained, that is, using the Mg(1)-substitution near Ag can bring considerable β_0 of 14300 au for all-metal electride molecule $CuAg@Ca_7Mg(1)$.

What is the origin of large first hyperpolarizability in new all-metal electride molecules is a meaningful question. From Table 3, CuAg@Ca$_7$Mg(1) with interaction between CuAg and Ca$_7$Mg(1) subunits and resulting multi-excess electrons has considerable β_0 of 14300 au. By contrast, its two isolated subunits CuAg and Ca$_7$Mg(1) without excess electron have small β_0 values of 844 and 35 au, respectively. The η value, a ratio of β_0 between a molecule and its subunits is β_0 (CuAg@Ca$_7$Mg(1))/[β_0(CuAg) + β_0(Ca$_7$Mg(1))] = 16, which clearly shows that the multi-excess electrons generated from subunit interaction is the fundamental origin of considerable β_0.

It is well known that besides electronic contribution, the effect of vibrations on the hyperpolarizabilities are also quite important.[81-83] Luis and coworkers[84] have already pointed that the vibrational hyperpolarizabilities exceed the corresponding static electronic property values by up to an order of magnitude for five selected electride molecules. Using Bishop and Kirtman theory[85,86] with double-harmonic approximation, we estimated the static vibrational first hyperpolarizabilities by high level MP2 method with the LANL2DZ for Cu and Ag and the 6-31G(3df) basis set for Be, Mg and Ca for these all-metal electride molecules. From Table 4, ratios ($\eta_{v/e}$) between β_0^v and β_0^e are 0.16-0.63, exhibiting large vibrational contribution. Therefore, total static first hyperpolarizability β_0^t including electronic and vibrational contributions for these all-metal electride molecules is obviously larger than its electronic contribution β_0.

The comparison of β_0 values between our all-metal electride molecules and previously reported organic and inorganic electride molecules is meaningful. Our 6500-14300 au is comparable to reported values: 7326 for an organic electride Li@calix[4]pyrrole,[10] 7197 for Cup···K$_3$O+···e@C$_{36}$F$_{36}^-$,[80] 10645 for LiCNLi@BNNT[75] and 12782 au for inorganic electride molecule Ca(NH$_3$)$_6$Na$_2$(b″).[76] Of course, there are also some reported electride molecules, which exhibited considerable β_0 values compared with our β_0 values of 6500-14300 au. For example, 8.89 ×10^5 au for a new inorganic electride compound M@r6−Al$_{12}$N$_{12}$,[87] a considerable 9.5 × 10^6 au for e$^-$@C$_{20}$F$_{19}^-$(CH$_2$)$^{4-}$NH$_2$···Na$^+$.[13] Obviously, the all-metal electride molecules have the larger β_0 values which are similar to those of some organic and inorganic electride molecules.

For the expectation of bulk material property, these all-metal electride molecules may act as building blocks. Figure 6 illustrates that structures and electronic first hyperpolarizabilities for polymers (block number n=1-3) of molecule CuAg@Ca$_8$. From Figure 6, a possible evolution of a molecule towards one-dimensional solid is exhibited and a favorite result is obtained that the electronic first hyperpolarizability increases sharply with increasing molecular unit number.

For NLO molecules, transparent region of electron spectrum is important. From Figure 7, the five all-metal electride molecules have the infrared (IR) transparent region of 1.3-6 μm, so these all-metal electride molecules are new IR NLO molecules.

4. Conclusions

It is well known that electride is a kind of interesting salt containing excess electron anions. Hitherto, extensive studies have been devoted to the organic electrides. Meanwhile, the recently developed inorganic electrides have also attracted great attention. However, the all-metal electride molecules have not been reported yet. It is worth noting that some polar intermetallic compounds containing excess electron anions and having an all-metal composition should belong to a new class of electrides. As a result, we propose a new concept referred to as all-metal electride. All-metal electride molecules $CuAg@Ca_7M$ (M = Be, Mg and Ca) are designed and researched in theory for the first time. In these molecules, the subunit interaction is interesting. Unusual all-metal polyanion $[Cu-Ag-Be/Mg]^{4-}$ or $[Cu-Ag]^{4-}$ pushes the remaining valence electrons of the Ca atoms to form the excess electrons (10/12). Then they can be described as salt-like $[(Ca^{2+})_7(CuAgM)^{4-}]+10e-$ (M = Be and Mg) and $[(Ca^{2+})_8(CuAg)^{4-}]+12e-$ (M = Ca). For these unusual molecules, a newfangled endohedral sandwich structure emerges. An inner all-metal polyanion is surrounded by 7 or 8 Ca^{2+} cations (as the counterions to prevent the Coulomb explosion of the polyanion), and the whole framework is surrounded by multi-excess electrons (10 or 12), which brings diverse covalent bonding modes including 2c-2e/3c-2e σ-bonding in the all-metal polyanions and weakly covalent bonding effect between Ca^{2+} cations due to surrounding the multi-excess electrons (special bonding electrons). The multi-excess electrons will also bring the electric conductivity of these NLO molecules. Thereout, a potential phenomemon – electric current effect on NLO responses may be predicted.

Especially, it is revealed that these all-metal electride molecules are a new class of NLO molecules with large electronic first hyperpolarizabilities (β_0) resulting from the involved multi-excess electrons. Based on the finding that the β_0 values depend on the atomic number and position of M, a new strategy to enhance β_0 is also obtained.

Considering a perspicacious analysis, the $CuAg@Ca_7Mg(1)$ has considerable β_0 (1.43×10^4 au) being 16 times the β_0 sum of two isolated CuAg and $Ca_7Mg(1)$ subunits, which sheds light on the fundamental origin of the considerable β_0, namely multi-excess electrons generated by the subunit interaction. These all-metal electride molecules have the IR transparent region of 1.3-6 μm and are new IR NLO molecules.

Besides electronic contribution β_0, the vibrational hyperpolarizabilities of these electride molecules are also estimated. We have reason to believe that total hyperpolarizability for these all-metal electride molecules are much larger than its large electronic contribution β_0.

An evolution of structure and property from a molecule towards solid material is significant. An initial discussion on a possible evolution of a molecule towards one-dimensional solid exhibits a favorite result that the electronic first hyperpolarizability increases sharply with increasing molecular unit number. Thus, a new research field in all-metal electride IR NLO molecule is opened.

Electronic supplementary information

The studies of the basis set effect care shown in Table S1 and Table S2. The binding energy (E_b) is shown in Table S3.

Notes and references

1. Y. Li, Z.-R. Li, D. Wu, R.-Y. Li, X.-Y. Hao and C.-C. Sun, *J. Phys. Chem. B.,* 2004, **108**, 3145.

2. W. Chen, Z.-R. Li, D. Wu, F.-L. Gu, X.-Y. Hao, B.-Q. Wang, R.-J. Li and C.-C. Sun, *J. Chem. Phys.,* 2004, **121**, 10489.

3. J. L. Dye, *Science* 1990, **247**, 663.

4. J. L. DYE, *Nature* 1993, **365**, 10.

5. J. L. Dye, *Inorg. Chem.,* 1997, **36**, 3816.

6. J. L. Dye, *Science* 2003, **301**, 607.

7. J. L. Dye, M. J. Wagner, G. Overney, R. H. Huang, T. F. Nagy and D. Tomanek, *J. Am. Chem. Soc.,* 1996, **118**, 7329.

8. A. S. Ichimura, J. L. Dye, M. A. Camblor, L. A. Villaescusa, *J. Am. Chem. Soc.,* 2002, **124**, 1170.

9. S. Matsuishi, Y. Toda, M. Miyakawa, K. Hayashi, T. Kamiya, M. Hirano, I. Tanaka and H. Hosono, *Science* 2003, **301**, 626.

10. K. Lee, S. W. Kim, Y. Toda, S. Matsuishi and H. Hosono, *Nature* 2013, **494**, 336.

11. W. Chen, Z.-R. Li, D. Wu, Y. Li, C.-C. Sun and F. L. Gu, *J. Am. Chem. Soc.,* 2005, **127**, 10977.

12. J.-J. Wang, Z.-J. Zhou, Y. Bai, Z.-B. Liu, Y. Li, D. Wu, W. Chen, Z.-R. Li, and C.-C. Sun, *J. Mater. Chem.,* 2012, **22**, 9652.

13. Y. Bai, Z.-J. Zhou, J.-J. Wang, Y. Li, D. Wu, W. Chen, Z.-R. Li and C.-C. Sun, *J. Phys. Chem. A,* 2013, **117**, 2835.

14. H.-L. Xu, Z.-R. Li, D. Wu, B.-Q. Wang, Y. Li, F. L. Gu, Y. Aoki, *J. Am. Chem. Soc.,* 2007, **129**, 2967.

15. R.-L. Zhong, H.-L. Xu, Z.-R. Li and Z.-M. Su, *J. Phys. Chem. Lett.,* 2015, **6**, 612.

16. H.-M. He, Z.-R. Li, Y. Li, W.-M. Sun, J.-J. Wang, J.-y. Liu and D. Wu, *J. Phys. Chem. C,* 2014, **118**, 23937.

17. Z.-Z. Luo, C.-S. Lin, W.-L. Zhang, H. Zhang, Z.-Z. He and W.-D. Cheng, *Chem. Mater.,* 2014, **26**, 1093.

18. T. K. Bera, J. I. Jang, J. B. Ketterson and M. G. Kanatzidis, *J. Am. Chem. Soc.,* 2008, **131**, 75.

19. Q. Zhang, I. Chung, J. I. Jang, J. B. Ketterson and M. G. Kanatzidis, *J. Am. Chem. Soc.,* 2009, **131**, 9896.

20. S. Banerjee, C. D. Malliakas, J. I. Jang, J. B. Ketterson and M. G. Kanatzidis, *J. Am. Chem. Soc.,* 2008, **130**, 12270.

21. X. Li, L. Kang, C. Li, Z. Lin, J. Yao and Y. Wu, *J. Mater. Chem. C,* 2015, **3**, 3060.

22. Z. Lin, C. Li, L. Kang, Z. Lin, J. Yao and Y. Wu, *Dalton Trans.,* 2015, **44**, 7404.

23. D.-M. Tan, C.-S. Lin, Z.-Z. Luo, H. Zhang, W.-L. Zhang, Z.-Z. He and W.-D. Cheng, *Dalton Trans.,* 2015, **44**, 7673.

24. H. Lin, L. Chen, L.-J. Zhou and L.-M. Wu, *J. Am. Chem. Soc.,* 2013, **135**, 12914.

25. M. H. Whangbo, C. Lee and J. Köhler, *Eur. J. Inorg. Chem.,* 2011, **2011**, 3841.

26. S. Scharfe, F. Kraus, S. Stegmaier, A. Schier and T. F. Faessler, *Angew. Chem. Int. Ed.,* 2011, **50**, 3630.

27. F. Gulo, J. Köhler, *Anorg. Allg. Chem.,* 2015, **641**, 557.

28. E. Y. Zakharova, N. A. Andreeva, S. M. Kazakov and A. N. Kuznetsov, *J. Alloy. Compd.,* 2015, **621**, 307.

29. E. Zurek, Y. Yao, *Inorg. Chem.,* 2015, **54**, 2875.

30. C. Lee, M. H. Whangbo and J. Köhler, *Anorg. Allg. Chem.,* 2010, **636**, 36.

31. N. Kazem, W. Xie, S. Ohno, A. Zevalkink, G. J. Miller, G. J. Snyder and S. M. Kauzlarich, *Chem. Mater.,* 2014, **26**, 1393.

32. C. B. Benda, M. Waibel and T. F. Fässler, *Angew. Chem. Int. Ed.,* 2015, **54**, 365.

33. M. M. Bentlohner, W. Klein, Z. H. Fard, L. A. Jantke and T. F. Fässler, *Angew. Chem. Int. Ed.,* 2015, **54,** 3748.

34. C. B. Benda, M. Waibel and T. F. Fässler, *Angew. Chem. Int. Ed.,* 2015, **54**, 522.

35. M.-H. Whangbo, C. Lee and J. Kohler, *Angew. Chem. Int. Ed.,* 2006, **45**, 7465.

36. J. Kohler, M.-H. Whangbo, *Solid State Sci.,* 2008, **10**, 444.

37. J. Kohler, M.-H. Whangbo, *Chem. Mater.,* 2008, **20,** 2751

38. F. Merlo, M. L. Fornasini, *Rev. Chim. Miner.,* 1984, **21**, 273.

39. R. Rand, L. Calvert, *J. Chem.,* 1962, **40**, 705.

40. C. J. Cramer, D. G. Truhlar, *Phys. Chem. Chem. Phys.,* 2009, **11**, 10757.

41. R. H. Petrucci,   W. S. Harwood, F. G. Herring, General Chemistry, 8th ed.; Prentice-Hall, 2002; pp. 341.

42. C. E. Housecroft, A. G. Sharpe, Inorg. Chem., 2nd ed.; Pearson Prentice-Hall, 2005; pp. 20.

43. S. Zhao, Z.-H. Li, W.-N. Wang, Z.-P. Liu, K.-N. Fan, Y. Xie and H. F. Schaefer III, *J. Chem. Phys.,* 2006, **124**, 184102.

44. S. Li, J. M. Hennigan, D. A. Dixon and K. A. Peterson, *J. Phys. Chem. A,* 2009, **113**, 7861.

45. M. Bühl, C. Reimann, D. A. Pantazis, T. Bredow and F. Neese, *J. Chem. Theory Comput.,* 2008, **4**, 1449.

46. E. Carter, K. M. Sharples, J. A. Platts and D. M. Murphy, *Phys. Chem. Chem. Phys.,* 2015, **17**, 11445.

47. A. Jiménez-Sánchez, B. Ortiz, V. O. Navarrete, J. C. Flores and N. Farfán, R. *Inorg. Chim. Acta.,* 2015, **429**, 243.

48. P. J. Hay, W. R. Wadt, *J. Chem. Phys.,* 1985, **82**, 270.

49. W. R. Wadt, P. J. Hay, *J. Chem. Phys.,* 1985, **82**, 284.

50. P. J. Hay, W. R. Wadt, *J. Chem. Phys.,* 1985, **82**, 299.

51. J. A. Bilbrey, A. H. Kazez, J. Locklin and W. D. Allen, *J. Comput. Chem.,* 2013, **34**, 1189.

52. P. Karamanis, *Int. J. Quantum Chem.,* 2012, **112**, 2115.

53. G. Maroulis, *Chem. Phys.,* 2003, **291**, 81.

54. G. Maroulis, *Chem. Phys. Lett.,* 1994, **226**, 420.

55. G. Maroulis, *Chem. Phys. Lett.,* 1996, **259**, 654.

56. G. Maroulis, *J. Chem. Phys.,* 1999, **111**, 583.

57. P. Karamanis, G. Maroulis, *Chem. Phys. Lett.,* 2003, **376**, 403.

58. M. Garcia-Borràs, M. Solà, J. M. Luis and B. Kirtman, *J. Chem. Theory Comput.,* 2012, **8**, 2688.

59. B. Champagne, E. Botek, M. Nakano, T. Nitta and K. Yamaguchi, *J Chem Phys.,* 2005, **122**, 114315.

60. M. Nakano, T. Nitta, K. Yamaguchi, B. Champagne and E. Botek, *J. Phys. Chem. A,* 2004, **108**, 4105.

61. S. Ito, M. Nakano, *J. Phys. Chem. C,* 2015, **119**, 148.

62. M. Nakano, R. Kishi, T. Nitta, T. Kubo, K. Nakasuji, K. Kamada, K. Ohta, B. t. Champagne, E. Botek and K. Yamaguchi, *J. Phys. Chem. A,* 2005, **109**, 885.

63. A. E. Reed, R. B. Weinstock and F. Weinhold, *J. Chem. Phys* 1985, **83**, 735.

64. S. F. Boys, F. d. Bernardi, *Mol. Phys.,* 1970, **19**, 553.

65. K. H. Weber, F. J. Morales and F.-M. Tao, *J. Phys. Chem. A,* 2012, **116**, 11601.

66. C. Møller, M. S. Plesset, *Phys. Rev.,* 1934, **46**, 618.

67. M. Head-Gordon, T. Head-Gordon, *Chem. Phys. Lett.,* 1994, **220**, 122.

68. Gaussian 09, Revision A.1, M. J. Frisch M. J. Frisch, G. W. Trucks, H. B. Schlegel, G. E. Scuseria, M. A. Robb, J. R. Cheeseman, G. Scalmani, V. Barone, B. Mennucci, G. A. Petersson, H. Nakatsuji, M. Caricato, X. Li, H. P. Hratchian, A. F. Izmaylov, J. Bloino, G. Zheng, J. L. Sonnenberg, M.; Ehara Hada, M., K.; Fukuda Toyota, R.;, J. Hasegawa, M. Ishida, T. Nakajima, Y. Honda, O. Kitao, H. Nakai, T. Vreven, J. A. Jr. Montgomery, J. E. Peralta, F. Ogliaro, M. Bearpark, J. J. Heyd, E. Brothers, K. N. Kudin, V. N. Staroverov, R. Kobayashi, J. Normand, K. Raghavachari, A. Rendell, J. C. Burant, S. S. Iyengar, J. Tomasi, M. Cossi, N. Rega, N. J. Millam, M. Klene, J. E. Knox, J. B. Cross, V. Bakken, C. Adamo, J. Jaramillo, R. Gomperts, R. E. Stratmann, O. Yazyev, A. J. Austin, R. Cammi, C. Pomelli, J. W. Ochterski, R. L. Martin, K. Morokuma, V. G. Zakrzewski, G. A. Voth, P. Salvador, J. J. Dannenberg, S.Dapprich, A. D.Daniels, O. Farkas, J. B. Foresman, J. V. Ortiz, J. Cioslowski, and D. J. FoxGaussian, Inc., Wallingford CT, 2009.

69. R. Dennington, T. Keith, J. G. V. Millam, GaussView, version 5, Semichem,Inc., Shawnee Mission, KS, 2009.

70.   J. C. Slater, *J. Chem. Phys.,* 1964, **41**, 3199.

71.   M. Pani, M. L. Fornasini, F. Merlo and Z. Krist-New. Cryst. St., 2007, **222**, 218.

72.   A. B. Nielsen, P. Hvelplund, B. Liu, S. B. Nielsen and S. Tomita, *J. Am. Chem. Soc.,* 2003, **125**, 9592.

73.   I. Last, Y. Levy and J. Jortner, *Natl. Acad. Sci.USA,* 2002, **99**, 9107.

74.   Z.-J. Zhou, H. Li, X.-R. Huang, Z.-J. Wu, F. Ma and Z.-R. Li, *Comput.Theor. Chem.,* 2013, **1023,** 99.

75.   R.-L. Zhong, H.-L. Xu, S. Muhammad, J. Zhang and Z.-M. Su, *J. Mater. Chem.,* 2012, **22**, 2196.

76.   W.-M. Sun, D. Wu, Y. Li, J.-Y. Liu, H.-M. He and Z.-R. Li, *Phys. Chem. Chem. Phys.,* 2015, **17**, 4524.

77.   Z.-B. Liu, Y.-C. Li, J.-J. Wang, Y. Bai, D. Wu and Z.-R. Li, *J. Phys. Chem. A.,* 2013, **117**, 6678.

78.   F. Lips, M. Hołyńska, R. Clérac, U. Linne, I. Schellenberg, R. Pöttgen, F. Weigend and S. Dehnen, *J. Am. Chem. Soc.,* 2012, **134**, 1181.

79.   J. Li, X. Li, H.-J. Zhai and L.-S. Wang, *Science* 2003, **299**, 864.

80.   J.-J. Wang, Z.-J. Zhou, Y. Bai, H.-M. He, D. Wu, Y. Li, Z.-R. Li and H.-X. Zhang, *Dalton Trans.,* 2015, **44**, 4207.

81.   J. M. Luis, J. Martí, M. Duran, J. L. Andrés and B. Kirtman, *J. Chem. Phys.,* 1998, **108**, 4123.

82.   B. Champagne, *Chem. Phys. Let.,* 1996, **261**, 57.

83.   D. M. Bishop, J. Pipin and B. Kirtman, *J. Chem. Phys.,* 1995, **102**, 6778.

84.   M. Garcia-Borràs, M. Solà, J. M. Luis and B. Kirtman, *J. Chem. Theory Comput.,* 2012, **8**, 2688.

85.   D. M. Bishop, B. Kirtman, *J. Chem. Phys.,* 1991, **95**, 2646.

86.   D. M. Bishop, B. Kirtman, *J. Chem. Phys.,* 1992, **97**, 5255.

87.   M. Niu, G. Yu, G. Yang, W. Chen, X. Zhao and X. Huang, *Inorg. Chem.*, 2013, **53**, 349.

Table 1 The Selected Distance (in Å), Followed by Their Wiberg Bond Index (WBI), at the PBE0 Level for the Intermetallic Compounds.

	Cu-Ag		Ca-Ag		Ca-Cu		Be/Mg-Ag		Be/Mg-Cu		Ca-Ca		Be/Mg-Ca	
A	2.594	0.79	3.231	0.45	2.989	0.47					(*1-3*) 3.874	0.28		
											(*3-4*) 4.085	0.19		
											(*1-8*) 4.156	0.20		
B	2.695	0.67	3.130	0.47	2.963	0.39	2.540	0.65	4.308	0.20	3.838	0.18	(*1-3*) 2.912	0.53
													(*1-6*) 3.089	0.43
													(*1-7*) 2.865	0.53
													(*1-8*) 3.040	0.45
C	2.594	0.73	3.111	0.61	2.928	0.50	2.932	0.44	4.083	0.19	3.868	0.27	(*1-3*) 3.372	0.41
													(*1-6*) 3.372	0.41
													(*1-7*) 3.789	0.23
													(*1-8*) 3.789	0.23
D	2.763	0.41	3.098	0.37	3.062	0.31	2.636	0.53	2.130	0.81	3.709	0.40	(*1-3*) 2.983	0.40
													(*3-4*) 2.998	0.39
													(*3-8*) 2.862	0.43
E	2.621	0.70	3.169	0.47	2.934	0.45	2.992	0.42	2.706	0.52	3.842	0.28	(*1-3*) 3.479	0.34
													(*3-4*) 3.707	0.22
													(*3-8*) 3.479	0.34

A, B, C, D, E are CuAg@Ca$_8$, CuAg@Ca$_7$Be(1), CuAg@Ca$_7$Mg(1), CuAg@Ca$_7$Be(3), CuAg@Ca$_7$Mg(3), respectively.

Table 2 The NBO Charges (q) and Valences (V) of Anion Subunits, Molecular Excess Electron

Number (N_e), the First Vertical Ionization Potential (VIP, in eV).

	q					V			Ne	VIP
	Cu	Ag	M	Cu-Ag	Cu-Ag-M	M	Cu-Ag	Cu-Ag-M		
CuAg@Ca$_8$	-1.223	-2.334		-3.557	-3.557		-4	-4	12	4.40
CuAg@Ca$_7$Mg(3)	-1.079	-2.250	-0.111	-3.329	-3.440	0	-4	-4	10	4.38
CuAg@Ca$_7$Be(3)	-0.341	-2.396	-0.896	-2.737	-3.633	-1	-3	-4	10	4.24
CuAg@Ca$_7$Be(1)	-0.839	-2.302	-0.971	-3.141	-4.112	-1	-3	-4	10	4.23
CuAg@Ca$_7$Mg(1)	-1.150	-2.373	-0.144	-3.523	-3.667	0	-4	-4	10	4.37

M = Be or Mg

Table 3 First Hyperpolarizability β_0 (au) at the MP2 level, HOMO–LUMO Gaps (in eV) at the MP2 level, Molecular Excess Electron Number (N_e), and Ratio of β_0 between a Molecule and its Subunits (η).

	β_0 (au)	Gap	N_e	η
CuAg@Ca$_8$	6500	3.524	12	
CuAg@Ca$_7$Mg(3)	7400	3.503	10	
CuAg@Ca$_7$Be(3)	9300	3.451	10	
CuAg@Ca$_7$Be(1)	12000	3.344	10	
CuAg@Ca$_7$Mg(1)	14300	3.586	10	16
CuAg	35			
Ca$_7$Mg(1)	844			

$\eta = \beta_0(\text{CuAg@Ca}_7\text{Mg(1)})/[\beta_0(\text{CuAg}) + \beta_0(\text{Ca}_7\text{Mg(1)})]$

18

Table 4 Static Electric First Hyperpolarizability β_0^e (au), Static Vibrational First Hyperpolarizability β_0^v (au) and Static Total First Hyperpolarizability β_0^t (au) at the MP2 level, and $\eta_{v/e}$ is ratio between β_0^v and β_0^e.

	β_0^e	β_0^v	β_0^t	$\eta_{v/e}$
CuAg@Ca$_8$	6500	1240	7740	0.19
CuAg@Ca$_7$Mg(3)	7400	1189	8589	0.16
CuAg@Ca$_7$Be(3)	9300	4774	14074	0.51
CuAg@Ca$_7$Be(1)	12000	7503	19503	0.63
CuAg@Ca$_7$Mg(1)	14300	2745	17045	0.19

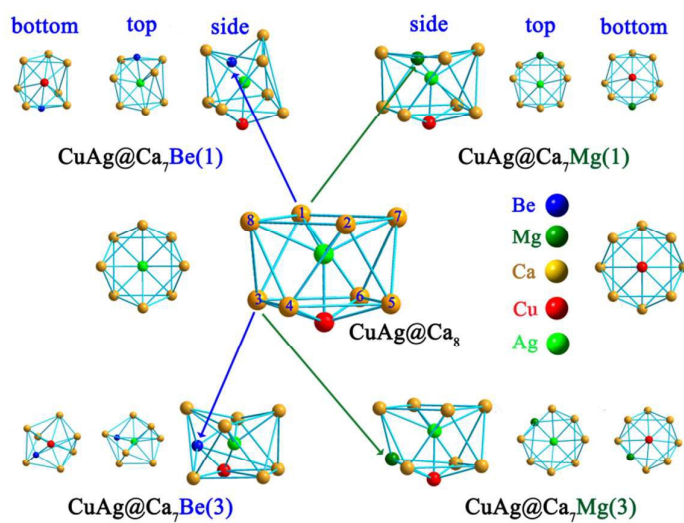**Figure 1** The optimized structures for the CuAg@Ca$_7$M (M = Be, Mg and Ca) molecules.

Figure 2 Occupied orbitals of multi-excess electrons in the all-metal electride compounds with all-metal polyanions. For CuAg@Ca7Mg(1), the orbital occupied one-excess electron is still double occupied with another non- excess electron.

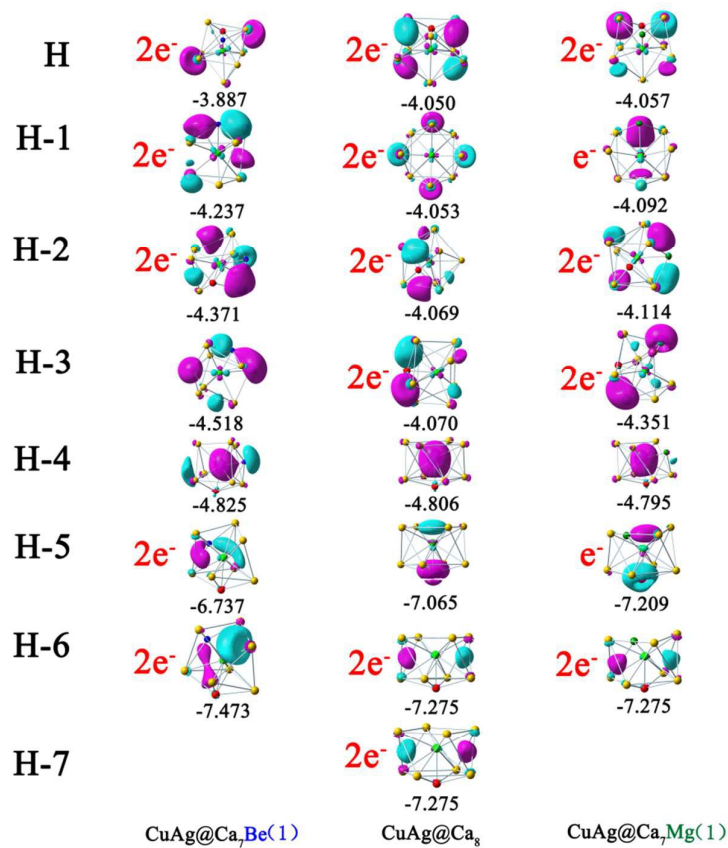H   2e⁻ ... 2e⁻ ... 2e⁻
                -3.887   -4.050   -4.057

H-1   2e⁻ ... 2e⁻ ... e⁻
                -4.237   -4.053   -4.092

H-2   2e⁻ ... 2e⁻ ... 2e⁻
                -4.371   -4.069   -4.114

H-3   ... 2e⁻ ... 2e⁻
                -4.518   -4.070   -4.351

H-4   ... ...
                -4.825   -4.806   -4.795

H-5   2e⁻ ... e⁻
                -6.737   -7.065   -7.209

H-6   2e⁻ ... 2e⁻ ... 2e⁻
                -7.473   -7.275   -7.275

H-7   ... 2e⁻ ...
                              -7.275

        CuAg@Ca₇Be(1)   CuAg@Ca₈   CuAg@Ca₇Mg(1)

Figure 3 The 2c-2e bonding σ-orbital in [Cu-Ag]$^{4-}$ and 3c-2e bonding σ-orbitals in [Cu-Ag-M]$^{4-}$ (M = Be and Mg).

CuAg@Ca$_8$
2c-2e

CuAg@Ca$_7$Be(1)

CuAg@Ca$_7$Be(3)

CuAg@Ca$_7$Mg(1)

CuAg@Ca$_7$Mg(3)

Cu-Ag-M chain
3c-2e

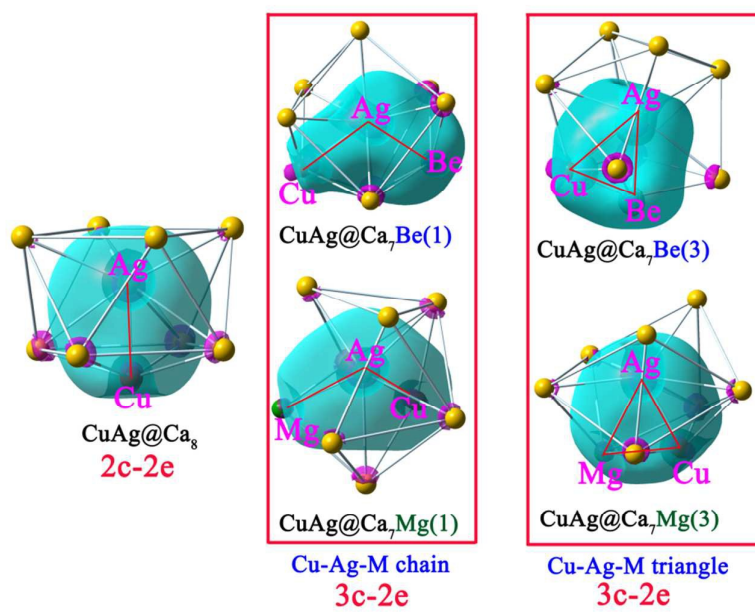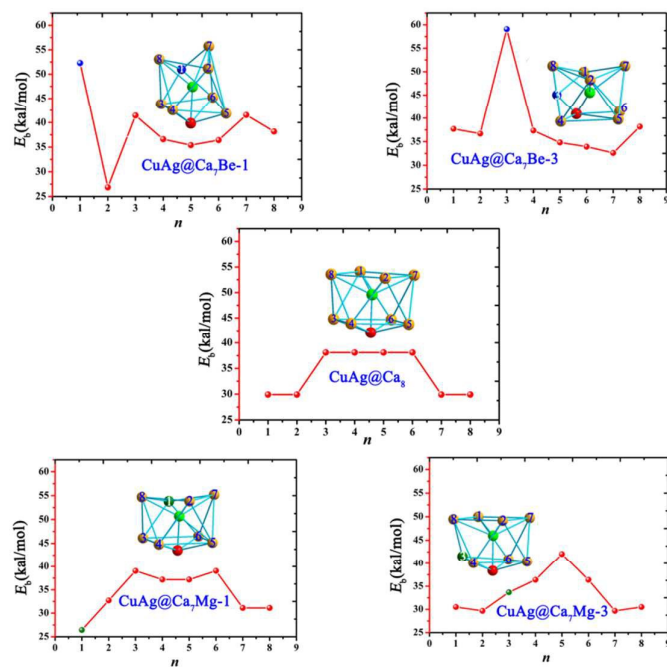Cu-Ag-M triangle
3c-2e

Figure 4 The binding energies of an atom in five all-metal electride molecules.

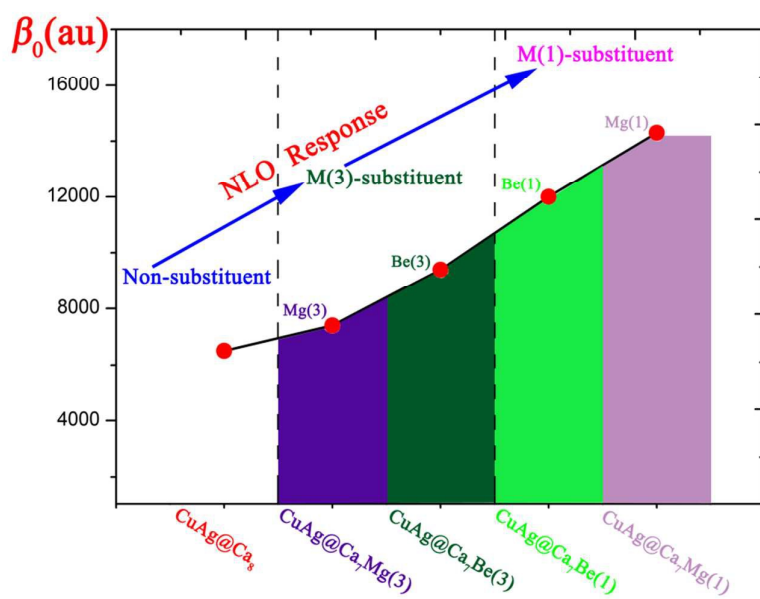**Figure 5** Be and Mg-substitution effects on β_0 in the all-metal electride molecules.

Figure 6 Structures and electronic first hyperpolarizabilities for polymers (block number n = 1-3) of molecule CuAg@Ca$_8$.
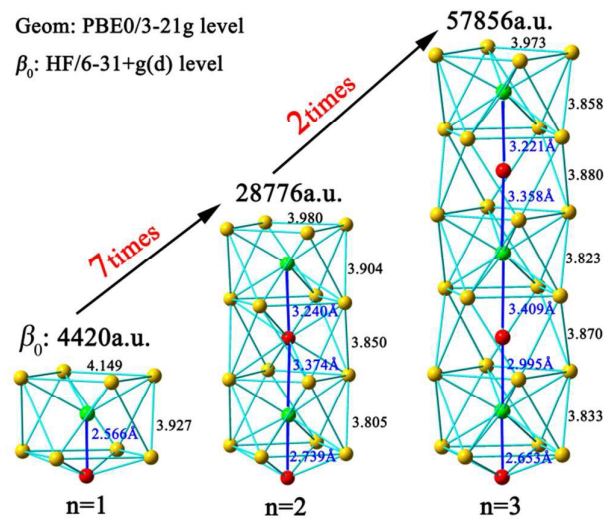
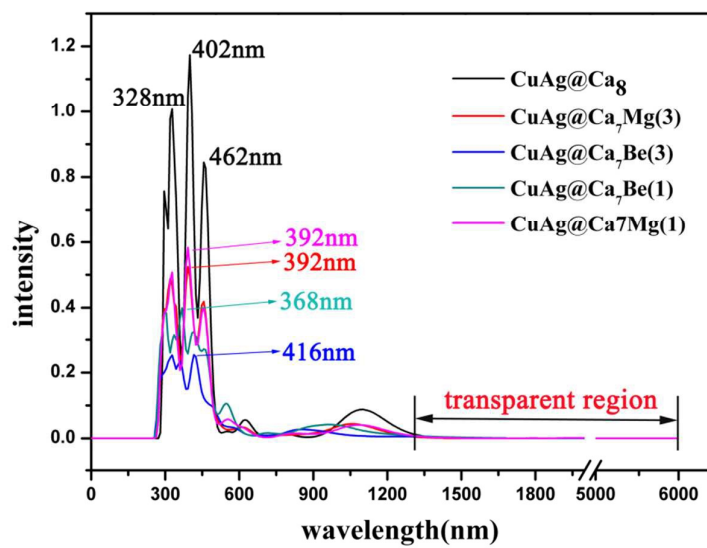**Figure 7** The electronic spectra of the all-metal electride compounds.

Table of Contents